Accelerated Publication

THE JOURNAL OF BIOLOGICAL CHEMISTRY
Vol. 276, No. 51, Issue of December 21, pp. 47767–47770, 2001

CaT1 and the Calcium Release-activated Calcium Channel Manifest Distinct Pore Properties*

Received for publication, October 18, 2001, and in revised form, October 29, 2001
Published, JBC Papers in Press, October 30, 2001,
DOI 10.1074/jbc.C100607200

Thomas Voets‡§, Jean Prenen‡, Andrea Fleig¶, Rudi Vennekens‡, Hiroyuki Watanabe‡, Joost G. J. Hoenderop‖, René J. M. Bindels‖, Guy Droogmans‡, Reinhold Penner¶, and Bernd Nilius‡

From the ‡Laboratory of Physiology, Catholic University of Leuven, B-3000 Leuven, Belgium, ¶Laboratory of Cell and Molecular Signalling, Center for Biomedical Research, The Queen's Medical Center and John A. Burns School of Medicine, University of Hawaii, Honolulu, Hawaii 96813, and the ‖Department of Cell Physiology, Institute of Cellular Signalling, University Medical Centre of Nijmegen, Nijmegen, The Netherlands

The calcium release-activated calcium channel (CRAC) is a highly Ca^{2+}-selective ion channel that is activated on depletion of inositol triphosphate (IP_3)-sensitive intracellular Ca^{2+} stores. It was recently reported that CaT1, a member of the TRP family of cation channels, exhibits the unique biophysical properties of CRAC, which led to the conclusion that CaT1 comprises all or part of the CRAC pore (Yue, L., Peng, J. B., Hediger, M. A., and Clapham, D. E. (2001) *Nature* 410, 705–709). Here, we directly compare endogenous CRAC with heterologously expressed CaT1 and show that they manifest several clearly distinct properties. CaT1 can be distinguished from CRAC in the following features: sensitivity to store-depleting agents; inward rectification in the absence of divalent cations; relative permeability to Na^+ and Cs^+; effect of 2-aminoethoxydiphenyl borate (2-APB). Moreover, CaT1 displays a mode of voltage-dependent gating that is fully absent in CRAC and originates from the voltage-dependent binding/unbinding of Mg^{2+} inside the channel pore. Our results imply that the pores of CaT1 and CRAC are not identical and indicate that CaT1 is a Mg^{2+}-gated channel not directly related to CRAC.

* This work was supported by the Belgian Federal Government, the Flemish Government, and the Onderzoeksraad Catholic University of Leuven (GOA 99/07, Fund for Scientific Research-Flanders (FWO) G.0237.95, FWO G.0214.99, FWO G.0136.00; Interuniversity Poles of Attraction Program, Prime Ministers Office IUAP Nr.3P4/23, and COF/96/22-A069); by Grant R7115 B0 from the "Alphonse and Jean Forton-Koning Boudewijn Stichting" (to B. N.); and by a grant from the Dutch Organization of Scientific Research (NWO-ALW 805-09.042). The costs of publication of this article were defrayed in part by the payment of page charges. This article must therefore be hereby marked "*advertisement*" in accordance with 18 U.S.C. Section 1734 solely to indicate this fact.

§ A postdoctoral Fellow of the Fund for Scientific Research-Flanders (Belgium) (FWO-Vlaanderen). To whom correspondence should be addressed. Tel.: 32-16-345738; Fax: 32-16-345991; Thomas.Voets@med.kuleuven.ac.be.

In non-excitable cells, calcium transients upon receptor stimulation generally consist of two phases: a rapid rise due to Ca^{2+} release from IP_3-sensitive[1] intracellular Ca^{2+} stores, which is followed by sustained Ca^{2+} entry through store-operated plasma membrane channels (1). Of all store-operated channels, CRAC is functionally the best described, but its molecular identity and the mechanism of its store-dependent activation remain elusive (2). Several members of the TRP family, a group of cation channels related to the *Drosophila* transient receptor potential (*trp*) gene product (3, 4), have been implicated in store-dependent Ca^{2+} influx (5–9), but until recently none of them was found to exhibit the unique biophysical properties of CRAC (3).

In a recent study, Yue *et al.* (10) reported that CaT1 (11), a TRP family member homologous to *Caenorhabditis elegans* OSM-9, manifests the pore properties and store dependence of CRAC, and it has been proposed that CaT1 comprises all or part of the CRAC pore (10, 12, 13). To further investigate this intriguing possibility, we made a direct comparison of CaT1, heterologously expressed in human embryonic kidney (HEK-293) cells, and endogenous CRAC in rat basophilic leukemia (RBL) cells. RBL cells were chosen because they were the source of the CaT1 clone used by Yue *et al.* (10) and have been widely used as a model system to study CRAC (2). We confirm the resemblance of currents through CRAC and CaT1 but additionally present a number of novel features that are incompatible with the proposed equality of the CaT1 and CRAC pores.

EXPERIMENTAL PROCEDURES

Cell Culture and Transfection—HEK-293 cells and RBL-2H3 cells were grown in Dulbecco's modified Eagle's medium containing 10% (v/v) human serum, 2 mM L-glutamine, 2 units/ml penicillin, and 2 mg/ml streptomycin at 37 °C in a humidity-controlled incubator with 10% CO_2. HEK-293 cells were transiently transfected with the pCINeo/IRES-GFP/mCaT1 vector using previously described methods (14), and electrophysiological recordings were performed between 8 and 24 h after transfection.

Electrophysiology—Patch clamp experiments were performed in the tight seal, whole-cell configuration at room temperature. Patch pipettes had DC resistances of 2–4 megaohms when filled with the standard intracellular solution containing (in mM): 145 cesium glutamate, 8 NaCl, 0, 3, or 10 $MgCl_2$, 3.3 $CaCl_2$, 10 EGTA, and 10 Hepes (pH 7.2). The free Ca^{2+} concentration in this solution was calculated to be 100 nM. The standard extracellular solution contained (in mM): 145 NaCl, 2.8 KCl, 10 CsCl, 10 $CaCl_2$, 2 $MgCl_2$, 10 glucose, and 10 Hepes (pH 7.4). The divalent-free (DVF) solution contained (in mM): 150 NaCl, 10 EDTA, 10 glucose, and 10 Hepes (pH 7.4). To test the monovalent cation permeability sequence, DVF solutions were used in which NaCl was equimolarly replaced by LiCl, CsCl, KCl, or NMDG chloride.

Unless indicated differently, currents were measured in response to voltage ramps (−100 to +100 mV in 100 ms) applied at a frequency of 0.5 Hz from a holding potential of 0 mV. Series resistances were between 3 and 10 megaohms and were compensated for 50–80%. Voltage errors were generally <10 mV. Currents were sampled at 10 kHz and filtered at 2 kHz using an eight-pole Bessel filter. For the accurate determination of the currents through CRAC, background currents measured under identical ionic conditions but before store depletion were subtracted. Averaged data are expressed as the mean ± S.E. from

[1] The abbreviations used are: IP_3, inositol triphosphate; CRAC, calcium release-activated calcium channel; HEK, human embryonic kidney; RBL, rat basophilic leukemia; DVF, divalent free; ECaC1, epithelial calcium channel 1; 2-APB, 2-aminoethoxydiphenyl borate; VOCC, voltage-operated calcium channel; NMDG, *N*-methyl-D-glucamine.

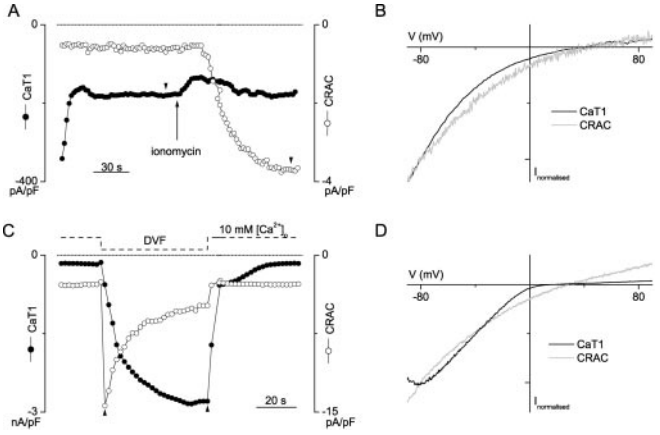

FIG. 1. **Comparison of the activation mechanism of CaT1 and CRAC and of their behavior in the absence of divalent cations.** *A*, time course of currents through CaT1 and CRAC at −80 mV in standard extracellular solution (10 mM Ca^{2+}). CaT1 is instantaneously activated, whereas CRAC is activated by brief (5 s) application of ionomycin (2 μM). Currents were elicited by linear voltage ramps (2 V/s) from −100 to +100 mV applied every 2 s from a holding potential of 0 mV. *B,* current-voltage relations for CaT1 and CRAC in 10 mM external Ca^{2+}. Traces were obtained in the experiments shown in *A* at the time points indicated by the *arrowheads*. For CRAC, the background current before application of ionomycin was subtracted. *C*, effect of switching from the standard extracellular solution to a DVF solution on currents through CaT1 and CRAC at −80 mV. *D,* current-voltage relations for CaT1 and CRAC in DVF solution. Traces were obtained in the experiments shown in *C* at the time points indicated by the *arrowheads*. For CRAC, the background current in DVF before store depletion was subtracted. In *panels B* and *D*, traces were normalized to the current at −80 mV.

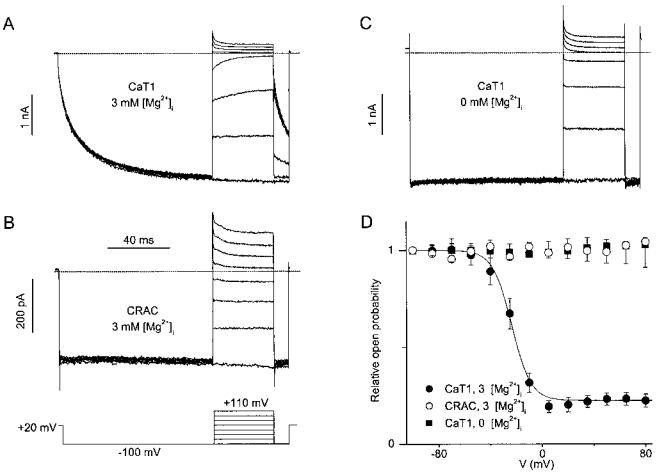

FIG. 2. **Comparison of the voltage dependence of CaT1 and CRAC.** *A* and *B,* current traces for CaT1 and CRAC in DVF solution in response to the voltage step protocol shown below. *C,* current traces for CaT1 when $MgCl_2$ was omitted from the intracellular solution. *D,* voltage dependence of the channel open probability for CaT1 and CRAC with 3 mM intracellular Mg^{2+} and for CaT1 in the absence of intracellular Mg^{2+} (n = 6–12). Currents were measured during the final step to −100 mV and normalized to the steady state current at this potential.

n cells. The significance of differences between means was evaluated using Student's unpaired t test.

RESULTS

Immediately after obtaining the whole-cell configuration, CaT1-transfected HEK-293 cells exposed to 10 mM extracellular Ca^{2+} and with intracellular Ca^{2+} buffered at 100 nM (to maintain full Ca^{2+} stores) displayed a large membrane current (Fig. 1, *A* and *B*). This current subsequently decayed to reach a lower, but still robust, steady state level (Fig. 1*A*). The CaT1-mediated current was strongly inwardly rectifying (Fig. 1*B*) and reversed at positive potentials (39 ± 7 mV; n = 18) in agreement with previous work (10). Depletion of intracellular Ca^{2+} stores with the Ca^{2+} ionophore ionomycin (2 μM) did not induce any store-dependent activation of CaT1 but instead caused a transient inhibition of the CaT1-current by 26 ± 4% (n = 8) (Fig. 1*A*). A similar inhibition by 30 ± 6% (n = 7) was observed when Ca^{2+} stores were passively depleted by application of the sarcoendoplasmic reticulum Ca^{2+}-ATPase inhibitor, 2,5-di-*t*-butyl-1,4-benzohydroquinone (20 μM). We attribute the inhibitory effect of store-depleting agents to an increase of intracellular Ca^{2+} as has been previously described for epithelial calcium channel (ECaC1; see Refs. 15 and 16), a close homologue of CaT1. Under identical intra- and extracellular ionic conditions, RBL-2H3 cells displayed only a very small background current that reversed at negative potentials (−41 ± 2 mV; n = 26). Depletion of Ca^{2+} stores by extracellular application of 2 μM ionomycin (Fig. 1*A*) or intracellular perfusion with IP_3 (20 μM; data not shown) activated CRAC, as indicated by the appearance of a Ca^{2+}-selective, inwardly rectifying current that reversed at positive potentials (42 ± 7 mV; n = 26) (Fig. 1*B*).

The permeability of both CaT1 and CRAC in the presence of extracellular Ca^{2+} is at least 100 times higher for Ca^{2+} than for Na^+, but removal of all divalent cations from the extracellular medium renders both channel pores highly permeable for monovalent cations (2, 10). This loss of selectivity is presumably because of the removal of divalents from negatively charged residues (aspartates or glutamates) lining the Ca^{2+}-selective pore (17), as has been previously shown for voltage-gated Ca^{2+} channels and for ECaC1 (18, 19). When switching from the normal extracellular solution containing 10 mM Ca^{2+} to a DVF solution, the CaT1-mediated current gradually increased following an exponential time constant of 9 ± 4 s (n = 14) (Fig. 1*C*). We interpret this time-dependent increase of the current as the slow removal of the Ca^{2+}-induced inactivation of CaT1, as has been previously demonstrated for its close homologue, ECaC1 (15, 16). After reaching its maximal amplitude, the monovalent CaT1 current remained stable for more than 15 min (Fig. 1*C* and data not shown). In contrast, the current through CRAC, when preactivated by ionomycin in the normal extracellular solution containing 10 mM Ca^{2+}, reached its maximal amplitude immediately after switching to DVF solution and decayed subsequently with a time constant of 12 ± 4 s (n = 17) (Fig. 1*C*).

Current-voltage relationships obtained during linear voltage ramps in DVF solutions revealed several significant differences between CaT1 and CRAC (Fig. 1*D*). First, the reversal potential for CaT1 (18 ± 2 mV; n = 8) was significantly less positive than for CRAC (45 ± 6 mV; n = 8). We examined whether this difference reflected different monovalent cation permeability profiles of the CaT1 and CRAC channel pores and found that, although both channels display a $Na^+ \approx Li^+ > K^+ > Cs^+ >$ NMDG permeability sequence, CRAC has a much lower relative Cs^+ permeability (P_{Cs}/P_{Na} = 0.48 ± 0.03 for CaT1 *versus* 0.12 ± 0.04 for CRAC; $p < 0.001$). Second, inward rectification was much more pronounced for CaT1 than for CRAC. The rectification score (defined as the ratio of the current amplitudes at potentials 40 mV negative and positive to the reversal potential) was 9.9 ± 1.1 (n = 15) for CaT1 compared with 1.5 ± 0.1 for CRAC (n = 19; $p < 0.001$). Third, the current-voltage relationship for CaT1 currents measured using the linear voltage ramp protocol displayed a negative slope at potentials below −80 mV, which was not observed for CRAC. As shown below, this negative slope originates from the time-dependent removal of intracellular Mg^{2+} block.

Monovalent cation currents through CaT1 activated during membrane hyperpolarization from +20 mV to −100 mV and deactivated during subsequent steps to less hyperpolarized

potentials (Fig. 2*A*). The fraction of open channels at the end of each voltage step was assessed from the initial current amplitude during a final step to −100 mV and exhibited a Boltzmann dependence on membrane potential (20), with a slope factor of 8 mV and half-maximal deactivation at −24 mV (Fig. 2*D*). This voltage dependence was abolished when Mg^{2+} was omitted from the intracellular solution (Fig. 2, *C* and *D*), indicating that the gating mechanism of CaT1 is a voltage-dependent block/unblock of the channel pore by intracellular Mg^{2+}. Using pipette solutions containing different concentrations of Mg^{2+}, we found that half-maximal block at 0 mV was achieved with ~200 μM intracellular Mg^{2+}. In contrast, monovalent cation currents through CRAC did not exhibit such voltage dependence (Fig. 2, *B* and *D*), not even with 10 mM intracellular Mg^{2+} ($n = 5$; data not shown).

It should be noted that CaT1 currents remained strongly inwardly rectifying in symmetric monovalent cation solutions and in the absence of intracellular Mg^{2+}, indicating that rectification represents an intrinsic pore property of CaT1. Moreover, the strong inward rectification and voltage-dependent Mg^{2+} block of CaT1 were preserved in cell-free inside-out patches (data not shown).

2-aminoethoxydiphenyl borate (2-APB), an inhibitor of IP_3 receptors, is known to inhibit store-dependent Ca^{2+} influx pathways in a variety of cells (21–25). We confirmed that 50 μM 2-APB caused a rapid and complete block of CRAC in RBL cells (Fig. 3*A*), which was voltage-independent (Fig. 3*B* and data not shown) and slowly reversible upon washout (Fig. 3*A*). The inhibitory effect of 2-APB on CRAC was dose-dependent with half-maximal inhibition at 5.5 μM (Fig. 3*D*). In contrast to a recent study (25), we did not observe a consistent initial increase in CRAC activity upon application of 2-APB. However, we cannot exclude the possibility that some 2-APB-dependent potentiation was masked by the rapid blocking effect of the drug. Although 2-APB has been shown to be membrane-permeable, two observations indicate that the target for 2-APB block of CRAC is exposed to the extracellular medium. First, the onset of block occurred with at time constant of ~2 s (Fig. 3*A*), which is almost as fast as block of CRAC by extracellular Zn^{2+}, Cd^{2+}, or La^{3+} (data not shown) and much faster than what has been reported for IP_3 receptor-mediated effects of 2-APB in intact cells (22). Second, dialysis of the cytoplasm with a pipette solution supplemented with 50 μM 2-APB did not markedly prevent activation of CRAC by ionomycin (data not shown; see also Ref. 23). From this we conclude that the interaction site for 2-APB is either on the extracellular part of the CRAC channel itself or at least closely associated therewith. In remarkable contrast with its inhibitory effects on CRAC, 50 μM 2-APB potentiated CaT1-mediated currents by ~25% (Fig. 3, *A* and *D*). The potentiating effect of 2-APB did not show marked voltage dependence (Fig. 3*C*), was fully reversible upon washout (Fig. 3*A*), and could be repeated several times in the same cell. A similar but less pronounced potentiation was obtained with 5 μM 2-APB (Fig. 3*D*). Application of 250 μM 2-APB also caused a potentiation of CaT1, which was mostly followed by a slow and moderate inhibition of the currents by ~20% and/or activation of linear leak currents. Thus, CRAC is at least 100 times more sensitive for 2-APB block than CaT1.

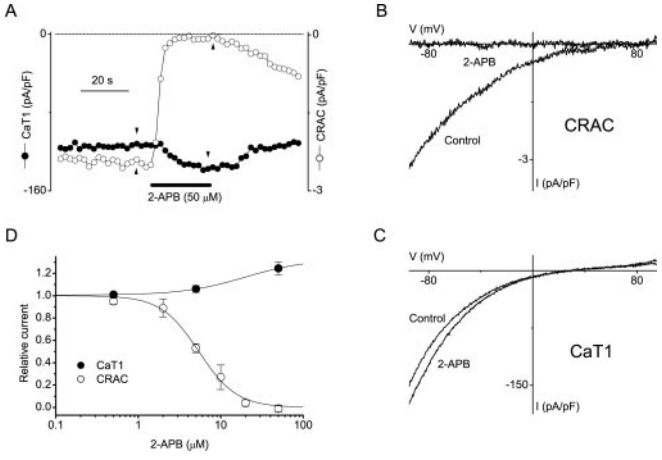

FIG. 3. **Comparison of the effects of 2-APB on CaT1 and CRAC.** *A*, time course of currents through CaT1 and CRAC measured at −80 mV in standard extracellular solution showing the effect of 50 μM 2-APB. *B* and *C*, current voltage relations for CRAC (*B*) and CaT1 (*C*) obtained during the experiments shown in *A* at the time points indicated by the *arrowheads*. *D*, dose-response relation for the effect of 2-APB on CaT1 and CRAC. Data points ($n = 4$–9) were normalized to the current measured in the absence of 2-APB.

According to Yue *et al.* (10), the properties of CaT1, notably its activation by active store depletion, were dependent on the expression level of the channel protein. Therefore, we wanted to make sure that the differences we observed between CaT1 and CRAC were independent on the number of CaT1 channels per cell. Like Yue *et al.* (10), we measured CaT1 currents within 12 h after transfection and selected for cells that had current densities below 100 pA/pF at −100 mV with 10 mM extracellular Ca^{2+} (mean peak amplitude, 78 ± 9 pA/pF; $n = 8$). Despite the fact that the average CaT1 current density in this group of cells was ~5 times lower than the overall average (356 ± 44 pA/pF; $n = 25$), they displayed all of the above

TABLE I
Summary of similarities and differences between CaT1 and CRAC

Properties of CaT1 and CRAC were determined in the present study unless indicated otherwise. pS, picosiemens.

	CaT1	CRAC (RBL cells)
Similarities		
Calcium selectivity	$P_{Ca}/P_{Na} > 100$[a]	$P_{Ca}/P_{Na} > 100$[b]
Anomalous mole fraction behavior	Yes[a]	Yes
Divalent permeability	$Ca^{2+} > Ba^{2+} \approx Sr^{2+} > Mg^{2+}$ [a]	$Ca^{2+} > Ba^{2+} \approx Sr^{2+} > Mg^{2+}$ [b]
Monovalent permeability	$Na^+ \approx Li^+ > K^+ > Cs^+$	$Na^+ \approx Li^+ > K^+ > Cs$
Effect of La^{3+}, Zn^{2+}, Cd^{2+}	Block	Block[c]
Single-channel conductance (150 Na^+)	42–58 pS[a]	55 pS[d]
Differences		
Effect of ionomycin	Inhibition	Activation
Current in DVF	Stable	Transient
Inward rectification in DVF	Strong	Weak
P_{Cs}/P_{Na}	0.48 ± 0.03	0.12 ± 0.04
Effect of intracellular Mg^{2+}	Voltage-dependent block	No effect
Effect of extracellular 2-APB	Potentiation	Inhibition

[a] From Ref. 10.
[b] From Ref. 32.
[c] From Ref. 33.
[d] From Ref. 34.

described CaT1 features: inhibition of 24% by 2 μM ionomycin ($n = 2$); strong inward rectification in DVF solution (rectification score, 12.7 ± 3.2; $n = 4$); relative Cs^+ permeability (P_{Cs}/P_{Na}) of 0.52 ± 0.06 ($n = 5$); voltage-dependent gating in the presence of intracellular Mg^{2+} with a slope factor of 8 mV and half-maximal deactivation at −25 mV ($n = 4$); potentiation to 121% of control by 50 μM 2-APB ($n = 2$). Thus, the biophysical and pharmacological properties that distinguish heterologously expressed CaT1 from endogenous CRAC in RBL cells are not influenced by the expression level of the CaT1 channel protein. Moreover, virtually identical results were obtained in CaT1-expressing Chinese hamster ovary cells (data not shown), indicating that the expression system does not significantly affect the properties of the CaT1 channel.

DISCUSSION

To evaluate the hypothesis that CaT1, a member of the TRP family of cation channels, constitutes all or part of CRAC, the calcium release-activated Ca^{2+} channel, we made a direct comparison of the biophysical and pharmacological properties of both channels under identical experimental conditions. At first sight, the similarities between CRAC and CaT1 (Table I) are indeed striking. However, it should be noted that many of the common characteristics of the CRAC and CaT1 pores (high Ca^{2+} selectivity; anomalous mole fraction effect; divalent and monovalent cation permeability sequence; block by inorganic cations; loss of selectivity in the absence of divalents; single-channel conductance to Na^+ in the range of 10–100 picosiemens) are not only shared by ECaC1 (15, 26, 27), which has a pore region virtually identical to the pore region of CaT1, but also shared to a large extent by voltage-operated Ca^{2+} channels (VOCCs) (17, 28–30), which have pore regions that are only weakly homologous to CaT1/ECaC1. In VOCCs and ECaC1, high Ca^{2+} selectivity depends on negatively charged amino acids (glutamates and/or aspartates) in the pore region (18, 19). It is believed that high affinity binding of Ca^{2+} ions to these sites prevents, by electrostatic repulsion, monovalent cations from passing through the pore while simultaneously allowing high rates of Ca^{2+} flux (17). Such a configuration implies that the pore becomes readily permeable to monovalent cations when the extracellular concentration of Ca^{2+} and other divalent cations is so low that the Ca^{2+}-binding sites are no longer occupied (20). Intermediate Ca^{2+} concentrations block monovalent permeation but yield only small Ca^{2+} fluxes. Thus, the conductance of these channels as a function of the extracellular Ca^{2+} concentration goes through a minimum, a phenomenon termed anomalous mole fraction behavior, which has been observed in VOCCs (17), ECaC1/CaT1 (10, 27), and CRAC (31). Moreover, because negatively charged Ca^{2+}-binding sites generally display a high affinity for transition metals such as Cd^{2+}, Zn^{2+}, or La^{3+} (20), it is not unexpected that these cations exert an inhibitory effect on the different Ca^{2+} selective channels. Thus, it appears that most of the pore properties common for CRAC and CaT1 are features inherent to all highly Ca^{2+}-selective pores in biological membranes.

As summarized in Table I, CaT1 differs from CRAC in RBL cells in the following salient features: effect of ionomycin-induced store depletion; current decay in DVF solution; relative permeability for Cs^+ *versus* Na^+; inward rectification; voltage-dependent block by intracellular Mg^{2+}; and effect of extracellular 2-APB. Obviously, some of these differences might be explained by cell-specific modulation of channel function. However, monovalent permeability, channel rectification, and voltage-dependent block represent biophysical properties that are directly related to the channel pore (20). Thus, our data demonstrate that the pore properties of CRAC and CaT1 are clearly distinct, thereby ruling out the possibility that CaT1 encompasses the full CRAC pore. We cannot definitely exclude the possibility that the CRAC pore consists of CaT1 plus an additional subunit, but this additional channel subunit would then have to abolish the intracellular Mg^{2+}-sensitivity of CaT1, provide for the 2-APB inhibition, and significantly alter the ion selectivity and inward rectification of the putative heteromultimeric channel. An alternative and presumably more likely explanation is that CRAC and CaT1 are two distinct channels with a number of overlapping properties but nevertheless encoded by different genes. In that case, we have provided a number of useful tools to discriminate between both channels in native tissue.

Acknowledgments—We thank A. Janssens, M. Crabbé, M. Schuermans, and H. Van Weijenbergh for excellent technical assistance.

REFERENCES

1. Clapham, D. E. (1995) *Cell* **80,** 259–268
2. Parekh, A. B., and Penner, R. (1997) *Physiol. Rev.* **77,** 901–930
3. Harteneck, C., Plant, T. D., and Schultz, G. (2000) *Trends Neurosci.* **23,** 159–166
4. Clapham, D. E., Runnels, L. W., and Strubing, C. (2001) *Nat. Rev. Neurosci.* **2,** 387–396
5. Zitt, C., Zobel, A., Obukhov, A. G., Harteneck, C., Kalkbrenner, F., Luckhoff, A., and Schultz, G. (1996) *Neuron* **16,** 1189–1196
6. Zhu, X., Jiang, M., Peyton, M., Boulay, G., Hurst, R., Stefani, E., and Birnbaumer, L. (1996) *Cell* **85,** 661–671
7. Philipp, S., Cavalie, A., Freichel, M., Wissenbach, U., Zimmer, S., Trost, C., Marquart, A., Murakami, M., and Flockerzi, V. (1996) *EMBO J.* **15,** 6166–6171
8. Philipp, S., Hambrecht, J., Braslavski, L., Schroth, G., Freichel, M., Murakami, M., Cavalie, A., and Flockerzi, V. (1998) *EMBO J.* **17,** 4274–4282
9. Freichel, M., Suh, S. H., Pfeifer, A., Schweig, U., Trost, C., Weissgerber, P., Biel, M., Philipp, S., Freise, D., Droogmans, G., Hofmann, F., Flockerzi, V., and Nilius, B. (2001) *Nat. Cell Biol.* **3,** 121–127
10. Yue, L., Peng, J. B., Hediger, M. A., and Clapham, D. E. (2001) *Nature* **410,** 705–709
11. Peng, J. B., Chen, X. Z., Berger, U. V., Vassilev, P. M., Tsukaguchi, H., Brown, E. M., and Hediger, M. A. (1999) *J. Biol. Chem.* **274,** 22739–22746
12. Putney, J. W., Jr. (2001) *Nature* **410,** 648–649
13. Petersen, O. H., and Fedirko, N. V. (2001) *Curr. Biol.* **11,** R520–523
14. Trouet, D., Nilius, B., Voets, T., Droogmans, G., and Eggermont, J. (1997) *Pflügers Arch. Eur. J. Physiol.* **434,** 632–638
15. Vennekens, R., Hoenderop, J. G., Prenen, J., Stuiver, M., Willems, P. H., Droogmans, G., Nilius, B., and Bindels, R. J. (2000) *J. Biol. Chem.* **275,** 3963–3969
16. Nilius, B., Prenen, J., Vennekens, R., Hoenderop, J. G., Bindels, R. J., and Droogmans, G. (2001) *Cell Calcium* **29,** 417–428
17. Hess, P., and Tsien, R. W. (1984) *Nature* **309,** 453–456
18. Yang, J., Ellinor, P. T., Sather, W. A., Zhang, J. F., and Tsien, R. W. (1993) *Nature* **366,** 158–161
19. Nilius, B., Vennekens, R., Prenen, J., Hoenderop, J. G., Droogmans, G., and Bindels, R. J. (2001) *J. Biol. Chem.* **276,** 1020–1025
20. Hille, B. (1992) *Ionic Channels of Excitable Membranes*, Sinauer Associates, Sunderland, MA
21. Ma, H. T., Patterson, R. L., van Rossum, D. B., Birnbaumer, L., Mikoshiba, K., and Gill, D. L. (2000) *Science* **287,** 1647–1651
22. Kukkonen, J. P., Lund, P.-E., and Akerman, K. E. O. (2001) *Cell Calcium* **30,** 117–129
23. Bakowski, D., Glitsch, M. D., and Parekh, A. B. (2001) *J. Physiol.* (*Lond.*) **532,** 55–71
24. Braun, F. J., Broad, L. M., Armstrong, D. L., and Putney, J. W., Jr. (2001) *J. Biol. Chem.* **276,** 1063–1070
25. Prakriya, M., and Lewis, R. S. (2001) *J. Physiol.* (*Lond.*) **536,** 3–19
26. Nilius, B., Vennekens, R., Prenen, J., Hoenderop, J. G., Bindels, R. J., and Droogmans, G. (2000) *J. Physiol.* (*Lond.*) **527,** 239–248
27. Vennekens, R., Prenen, J., Hoenderop, J. G., Bindels, R. J., Droogmans, G., and Nilius, B. (2001) *J. Physiol.* (*Lond.*) **530,** 183–191
28. Hess, P., Lansman, J. B., and Tsien, R. W. (1986) *J. Gen. Physiol.* **88,** 293–319
29. Lansman, J. B., Hess, P., and Tsien, R. W. (1986) *J. Gen. Physiol.* **88,** 321–347
30. Carbone, E., and Lux, H. D. (1987) *J. Physiol.* (*Lond.*) **386,** 571–601
31. Kerschbaum, H. H., and Cahalan, M. D. (1998) *J. Gen. Physiol.* **111,** 521–537
32. Hoth, M., and Penner, R. (1992) *Nature* **355,** 353–356
33. Hoth, M., and Penner, R. (1993) *J. Physiol.* (*Lond.*) **465,** 359–386
34. Kerschbaum, H. H., and Cahalan, M. D. (1999) *Science* **283,** 836–839